Conceptual model and experimental framework to determine the contributions of direct and indirect photoreactions to the solar disinfection of MS2, phiX174, and adenovirus

UNIVERSITÀ DEGLI STUDI DI TORINO

Environmental Science & Technology, 49, 2015, 334-342

DOI: 10.1021/es504764u

Contributions of direct and indirect photoreactions to the solar disinfection of MS2, phiX174 and adenovirus in surface waters

Michael J. Mattle[1], Davide Vione[2] and Tamar Kohn[1]*

[1]Laboratory of Environmental Chemistry, School of Architecture, Civil and Environmental Engineering (ENAC), École Polytechnique Fédérale de Lausanne (EPFL), CH-1015 Lausanne, Switzerland

[2]Dipartimento di Chimica, Università di Torino, Via P. Giuria 5, 10125, Torino, Italy

*Corresponding author email address: tamar.kohn@epfl.ch

Abstract

Sunlight inactivates waterborne viruses via direct (absorption of sunlight by the virus) and indirect processes (adsorption of sunlight by external chromophores, which subsequently generate reactive species). While the mechanisms underlying these processes are understood, their relative importance remains unclear. This study establishes an experimental framework to determine the intrinsic virus parameters associated with their susceptibility to solar disinfection, and proposes a model to estimate disinfection rates and to apportion the contributions of different processes. Quantum yields of direct inactivation were determined for three viruses (MS2, phiX174 and adenovirus), and second-order rate constants associated with indirect inactivation by four reactive species ($^1O_2$, $OH^{\cdot}$, $CO_3^{\cdot-}$, and triplet states) were established. PhiX174 exhibited the greatest quantum yield ($1.42 \cdot 10^{-2}$), indicating that it is more susceptible to direct inactivation than MS2 ($2.9 \cdot 10^{-3}$) or adenovirus ($2.5 \cdot 10^{-4}$). Second-order rate constants with $^{\bullet}OH$ ranged from $1.7 \cdot 10^9$ to $7.0 \cdot 10^9$ $M^{-1}s^{-1}$ and followed the sequence MS2>adenovirus>phiX174. A predictive model based on these parameters accurately estimated solar disinfection of MS2 and phiX174 in a natural water sample, and approximated that of adenovirus within a factor three. Inactivation mostly occurred by direct processes, though indirect inactivation by $^1O_2$ also contributed to the disinfection of MS2 and adenovirus.

Introduction

Waterborne pathogens continue to pose a public health challenge throughout the world. Pathogens can reach surface waters via direct input or the discharge of insufficiently treated sewage. Several factors have been identified that influence pathogen fate in surface waters: temperature, sedimentation, pH, biological disinfection (e.g., grazing by microorganisms) and sunlight.[1,2] Among these factors, sunlight is often considered the most important,[1,3–10] and several low-cost water treatment techniques, including waste stabilisation ponds (WSPs) and solar disinfection for drinking water (SODIS), rely on sunlight for disinfection.[2,8,11,12]

Most studies on solar disinfection to date have focused on bacterial indicator organisms, such as *E. coli* and faecal coliforms. Less is known about whether these results also hold for pathogenic viruses and parasites.[1] A number of studies have indicated that viruses are generally more resistant to sunlight-mediated inactivation than bacteria.[7,10,13,14] Nevertheless, to date only few studies have investigated mechanisms of removal or inactivation of viruses in surface waters.[2]

Solar disinfection of viruses can occur by direct or indirect inactivation processes. Direct inactivation (sometimes referred to as endogenous inactivation) involves the absorption of UVB light by the viral genome, which leads to its degradation. In indirect (or exogenous) inactivation, light in the UVB/A and visible range is absorbed by sensitizers in the water, such as organic matter (OM), nitrate, nitrite or iron-containing complexes. The excited sensitizers then generate reactive species including singlet oxygen ($^1O_2$), hydroxyl radicals ($OH^{\cdot}$), triplet state OM (^3OM) or carbonate radicals ($CO_3^{\cdot-}$),[15,16] which can inactivate viruses. The relative contribution of direct and indirect inactivation depends on the virus under consideration and the solution conditions. For example, Davies-Colley et al. [17] showed that in WSPs, F-RNA phages were inactivated by UVB/UVA and visible light, whereas F-DNA phages were mainly inactivated by UVB. They concluded that the inactivation of the former includes a significant indirect contribution, whereas the latter are primarily inactivated directly.[3] Furthermore, $^1O_2$ was suggested as the most important reactive species to cause inactivation of MS2 coliphage in WSP water.[18] Apart from $^1O_2$, several studies focussed on the effects of organic matter or different water origins on solar disinfection.[19–21] These studies showed that organic matter influences virus inactivation, but each virus responds differently to varying water compositions. Both $^1O_2$ and ^3OM have been correlated with virus inactivation[21,22]. However, different inactivation pathways may occur simultaneously, and no attempt has been made to determine the contribution of the different pathways.

The goal of this work was to elucidate the contribution of direct inactivation and the different reactive species to total solar virus disinfection in surface waters in general, and in a WSP sample in

particular. MS2, a single-stranded (ss)RNA phage, phiX174 a ssDNA phage and human adenovirus type 2, a double-stranded (ds) DNA virus, served as the test organisms. MS2 is susceptible to reactive species but relatively resistant to direct inactivation, while phiX174 exhibits the opposite behaviour.[23] Adenovirus is expected to have a similar solar disinfection behaviour as MS2; it is one of the most resistant viruses to UV disinfection,[24–26] but it is susceptible to inactivation by $^1O_2$.[27]

In controlled experimental solutions, inactivation quantum yields of these viruses were determined as a proxy of direct inactivation, and second-order inactivation rate constants associated with indirect inactivation were obtained for four reactive species ($^1O_2$, $OH^{\cdot}$, $CO_3^{\cdot-}$, and triplet states). Using these parameters, a simple, predictive model of solar virus disinfection was established, which allowed us to estimate inactivation rate constants in an environmental WSP sample and apportion the contributions of different processes and reactive species involved.

Experimental section

Chemicals and Organisms

The chemicals, organisms and culturing methods used are described in the Supporting Information (hereafter SI).

Experimental approach

Four sets of experiments were conducted. First, direct inactivation of the three viruses was studied under a solar simulator, and the inactivation quantum yields were computed. Second, the second-order rate constants for the inactivation of the three viruses by four reactive species ($^1O_2$, $OH^{\cdot}$, $CO_3^{\cdot-}$, and triplet states) were determined. Third, steady-state concentrations of the reactive species were measured in a WSP sample under simulated sunlight using selective probe compounds. These data, jointly with the inactivation quantum yields and second-order rate constants, were used to predict virus inactivation in the WSP sample. Finally, solar disinfection of the viruses in the WSP water was measured under simulated sunlight, and was compared to the predicted inactivation.

Solar disinfection experiments were conducted in a thermostatic bath (23 ± 2°C) in 30 mL closed Pyrex cells containing 20 mL of solution (solution depth: 1.6 cm), unless stated otherwise. The light transmission spectrum of the Pyrex cells is shown in the SI (Fig. S7). Experimental solutions were either autoclaved or filtered through 0.20 µm or 0.45 µm pore size filters (Whatman™). Samples were irradiated by different light sources and in the presence of different sensitizers (discussed below). Aliquots (150 or 200 µL) were withdrawn periodically, added to 450 µL phosphate-buffered saline (PBS, for phages) or 800 µL Dulbecco's modified Eagle's medium (DMEM, for adenovirus), and the remaining infective virus concentration was enumerated. Control experiments were conducted in WSP samples in the dark, as well as in PBS under irradiation, to assess the extent of

dark and direct virus inactivation or probe compound degradation under the experimental conditions used herein.

Quantum yields for direct inactivation

The inactivation quantum yield, $\Phi_{v,p}$, compares the number of inactivated viruses with the number of photons absorbed over time by a viral solution. Specifically, it corresponds to the ratio of the direct virus inactivation rate and the photon absorption rate.

Direct virus inactivation rates were determined in 20 mL PBS samples irradiated by a Sun 2000 Solar Simulator (ABET Technologies, Milford, Connecticut) equipped with a 1000 W Xe lamp, an Air Mass (AM) 1.5 filter and a 2 mm thick Atmospheric edge (AE) filter to mimic the solar radiation spectrum (SI Fig. S7). The fluence rate of the simulator was measured by an ILT 900-R (ruggedized wideband) spectroradiometer (International Light Technologies). As the sensitivity of the spectroradiometer in the UVB range was low, the AE filter was removed from the simulator to measure the spectrum. The fluence in the presence of the AE filter was then computed from the measured lamp output with the AM 1.5 filter only, multiplied by the transmission spectrum of the AE filter.

For phiX174, additional experiments were conducted in open beakers with the same surface area as the Pyrex cells. Adenovirus experiments were carried out in competition with MS2 and in the absence of the AE filter to reduce the experimental time. All experimental conditions and data pertaining to the measurement of the inactivation quantum yields are summarized in the SI (Tables S13 and S14).

To determine the rate of photon absorption, the absorption spectrum for a single virus had to be established. For this purpose, it was assumed that within the wavelength range of solar radiation, light absorption by viruses is dominated by the genomes, whereas absorption by proteins is negligible in comparison. The absorbance spectrum of DNA and RNA both exhibit a pronounced peak around 260 nm. For a given virus, the absolute absorbance at 260 nm can be calculated by multiplying the weight of the genome with the known, weight-normalized extinction coefficient of the respective genome type at 260 nm (ε(260 nm)). The values of ε(260) for ssRNA, ssDNA and dsDNA are 0.025, 0.027, and 0.020 $(\mu g/mL)^{-1}cm^{-1}$,[28] respectively. The weights of the genomes of MS2, phiX174 and adenovirus are $1.91 \cdot 10^{-12}$ µg,[29] $2.77 \cdot 10^{-12}$ µg and $3.70 \cdot 10^{-11}$ µg, respectively.[30–32] The absorption spectrum of each virus at wavelength > 260 nm was then determined by taking into account the shape of the absorption spectrum of a virus solution. For MS2 and phiX174, this was done by measuring the UV/vis absorbance of a purified virus stock. In the case of adenovirus, the stock was not sufficiently pure to obtain a reliable measurement, therefore the shape of the phiX174 spectrum (also a DNA virus) was used. The measured spectrum was normalized such that the absorbance at 260 nm corresponded to the calculated one. Finally, a Gaussian distribution around the

peak at 260 nm was fitted to the absorbance spectra from 280 nm onwards to remove any measurement noise from the baseline. This yielded the extinction coefficients for a single virus, $\varepsilon_{virus}(\lambda)$ [mL virus $^{-1}$cm^{-1}] (SI Table S3).

The rate of photon absorption by the viruses (P_{α}^{virus} $[photons\ s^{-1}mL^{-1}]$) was computed analogously to the specific rate of light absorption of an organic chemical in a light-absorbing solution,[33,34] according to equation 1 (SI Fig. S8)

$$P_{\alpha}^{virus} = \int_{\lambda} \frac{p^0(\lambda)\varepsilon_{virus}(\lambda)c_{virus}}{\left(b \cdot \alpha_{solution}(\lambda)\right)\left(1 - 10^{-\alpha_{solution}(\lambda)b}\right)d} \lambda \quad \text{(EQ. 1)}$$

Here $p^0(\lambda)$ is the incident photon flux density [photons s^{-1} cm^{-2} nm^{-1}], $\varepsilon_{virus}(\lambda)$ the virus extinction coefficient in [mL virus^{-1} cm^{-1}], c_{virus} the virus concentration in [virus mL^{-1}], $\alpha_{solution}(\lambda)$ the total absorbance of the solution in [cm^{-1}], and b the optical path length in the reactor [cm].

Finally, Φ_v was determined by dividing the initial virus inactivation rate $R_{virus}^0 = -dc_{virus}^0/dt$ by the rate of photons absorbed by the viruses

$$\Phi_v = R_{virus}^0 / P_{\alpha}^{virus} \quad \text{(EQ. 2)}$$

Second-order inactivation rate constants

Unless noted otherwise, second-order rate constants for the inactivation of MS2 and in part for phiX174 by reactive species $(k_{virus-reactive\ species})$ were determined in competition experiments with organic probe compounds with known corresponding second-order degradation rate constants $(k_{probe-reactive\ species})$. For adenovirus and in part for phiX174, experiments were conducted in competition with MS2. This latter approach was chosen for two reasons: first, it allowed us to directly assess the validity of using MS2 as a surrogate of adenovirus. Second, it circumvented the need for probe compound analysis by HPLC (solutions containing infective adenovirus could not be analysed by HPLC due to biosafety considerations). During each experiment, aliquots were removed periodically to enumerate infectious viruses as discussed above. Simultaneously, when relevant, 1-1.5 mL aliquots were taken for probe compound quantification and were analysed by HPLC (see SI for details). All experimental conditions and data pertaining to the measurement of second-order inactivation rate constants are summarized in the SI (Tables S5-S12).

Hydroxyl radical. $OH^{\cdot}$ was generated by nitrate photolysis under a UVB lamp (Philips UVB Narrowband TL 20W/01, intensity: 0.95 ± 0.05 W/m^2). Experiments were conducted with 20 mL of 10 or 50 mM nitrate and 5 mM phosphate at pH 7.5. The second-order rate constant of MS2 inactivation by $OH^{\cdot}$ was determined in a competition reaction with 20 µM tryptophan. Hereby, the

inactivation of MS2 and the degradation of tryptophan were measured simultaneously in the same reactor. The corresponding inactivation or degradation rates can be formulated as

$$dc_{MS2}/dt = -k_{MS2-OH^{\cdot}} \cdot c_{OH^{\cdot},SS} c_{MS2} = -k_{app,MS2} c_{MS2} \quad \textbf{(EQ. 3)}$$

$$dc_{tryp}/dt = -k_{tryp-OH^{\cdot}} \cdot c_{OH^{\cdot},SS} c_{tryp} = -k_{app,tryp} c_{tryp}. \quad \textbf{(EQ. 4)}$$

Where $k_{MS2-OH^{\cdot}}$ is the second-order rate constant for the inactivation of MS2, $k_{tryp-OH^{\cdot}}$ is the second-order rate constant for the degradation of tryptophan, $c_{OH^{\cdot},SS}$ is the $OH^{\cdot}$ steady-state concentration, and c_{MS2} and c_{tryp} are the infective MS2 and the tryptophan concentrations at time t. $k_{MS2-OH^{\cdot}}$ could then be determined from the ratio of the respective pseudo-first-order degradation rate constants (k_{app}):

$$k_{MS2-OH^{\cdot}} = \frac{k_{app,MS2}}{k_{app,tryp}} k_{tryp-OH^{\cdot}}. \quad \textbf{(EQ. 5)}$$

Where ($k_{tryp-OH^{\cdot}}$) corresponds to $1.3 \cdot 10^{10}$ $M^{-1}s^{-1}$.[35] The presence of tryptophan suppressed the steady-state concentration of $OH^{\cdot}$, such that the inactivation of phiX174, a much more sensitive organism toward UVB inactivation, became largely dominated by direct inactivation in the same set-up. Hence, inactivation of phiX174 and adenovirus was subsequently determined in a similar manner by using the competition with MS2, without the addition of tryptophan.

Carbonate radical. $CO_3^{\cdot-}$ was generated by scavenging $OH^{\cdot}$ via the addition of (bi)carbonate (100 mM) to the nitrate solution described above. The pH was adjusted to 9.2 to maximize the concentration of CO_3^{2-}, while avoiding virus inactivation due to elevated pH. $k_{MS2-CO_3^{\cdot-}}$ was determined in a competition reaction with 10 µM tyrosine in the same manner as described for $OH^{\cdot}$ (Eq. 3-5). Under our experimental conditions, the concentration of the $CO_3^{\cdot-}$ was 3900 times higher than that of the $OH^{\cdot}$, such that 98 % of the degradation of tyrosine could be attributed to $CO_3^{\cdot-}$ ($k_{tyrosine-CO_3^{\cdot-}} = 1.4 \cdot 10^8$ $M^{-1}s^{-1}$),[36] and only 2 % to $OH^{\cdot}$ ($k_{tyrosine-OH^{\cdot}} = 1.3 \cdot 10^{10}$ $M^{-1}s^{-1}$).[35]

As for the inactivation studies with $OH^{\cdot}$, inactivation of phiX174 and adenovirus were determined in competition experiments with MS2 without the addition of tyrosine. Calculations carried out with the derived virus rate constants confirmed that all viruses in the studied systems were mostly inactivated by $CO_3^{\cdot-}$ and not (or to a far lesser extent) by $OH^{\cdot}$.

Singlet oxygen. $^1O_2$ was produced by visible light excitation of Rose Bengal (RB) by a yellow lamp (TL D 18W/16, intensity: 0.022 ± 0.02 W/m^2). The experiments were performed in 20 mL phosphate buffer (PB, 5 mM phosphate at pH 7.5), which was spiked with RB (10 µM). Furfuryl alcohol (FFA) was used as a $^1O_2$ probe. However, the FFA degradation products can cause virus inactivation. Therefore, virus inactivation by $^1O_2$ was studied in the absence of FFA and the degradation of the

latter was measured in separate reactors containing identical experimental solutions including viruses. This approach is possible because the low FFA concentration used (50 µM) did not affect the steady-state concentration of $^1O_2$, which is mostly scavenged by thermal inactivation upon collision with the solvent (lifetime around 4 µs).[34] $k_{MS2-^1O_2}$ and $k_{phiX174-^1O_2}$ were calculated in an analogous way as described in Eq. 3-5 using the second-order degradation rate constant $k_{FFA-^1O_2} = 1.2 \cdot 10^8$ $M^{-1}s^{-1}$.[37] $k_{adeno-^1O_2}$ was measured in competition experiments with MS2.

In order to discriminate between virus inactivation by $^1O_2$ versus excited-state RB, additional experiments with both MS2 and phiX174 were conducted in D_2O. D_2O is a 13-fold weaker quencher of $^1O_2$ than H_2O,[38] therefore the steady-state concentration of $^1O_2$ increases while the steady-state concentration of excited RB is not affected.

Triplet state OM. Inactivation by triplet states was studied by UVA excitation (Philips TL-K UVA 40W, intensity: 8.7 ± 0.4 W/m^2) of anthraquinone-2-sulfonate (AQ2S, 50 µM in PB), which served as a proxy ^{3}OM. The advantage of using AQ2S is that it produces neither $^1O_2$ nor $OH^{\cdot}$.[39,40] The steady-state concentration of the AQ2S triplet state (^{3}AQ2S) was determined indirectly by following the AQ2S degradation via HPLC, as described in the SI on the basis of a kinetic model reported elsewhere.[40a] $k_{MS2-AQ2S}$ and $k_{phiX174-AQ2S}$ were determined by dividing the pseudo-first order degradation rate constant $k_{app,virus}$ by the steady-state concentration of ^{3}AQ2S. To rule out a possible influence of the viruses on the ^{3}AQ2S steady-state concentration, experiments were conducted at varying initial phage concentrations (see SI, Fig. S2 and Table S11). $k_{adeno-AQ2S}$ was measured in competition experiments with MS2.

Virus inactivation in WSP water

In order to validate the second-order rate constants and inactivation quantum yields in environmental solutions, inactivation of viruses was studied in an environmental water sample, specifically in WSP water. Water was collected from the third pond (second maturation pond) of the WSP in Vuiteboeuf, Switzerland. The absorbance spectrum of the water is shown in the SI (Fig. S9). The WSP water had a pH of 8.3, a non-purgeable organic matter content of 14.4 mg C L^{-1} and a dissolved organic carbon content of 52 mg L^{-1} (determined by Shimadzu TOC-V_{CPH} analyzer), as well as 3.5 mg nitrate L^{-1} and 0.6 mg nitrite L^{-1} (determined by SEAL AutoAnalyzer 3 colorimeter). The sample was filtered through 0.45 µm pore size membranes and was stored at -22 °C or at 4 °C when analysed within two weeks.

Virus inactivation in the WSP sample was measured under simulated sunlight in Pyrex cells containing 20 mL WSP water. All experimental conditions and data pertaining to the inactivation measurement in the WSP water are summarized in the SI (Tables S13 and S15).

Steady-state concentrations of reactive species in irradiated WSP water

The steady-state concentrations of reactive species were measured with selective probe compounds in parallel Pyrex reactors containing WSP water, as described elsewhere.[41] In brief, the $OH^{\cdot}$ concentrations were measured by monitoring the production of phenol from benzene ($k_{benzene-OH^{\cdot}}$ = $7.8 \cdot 10^9$ $M^{-1}s^{-1}$),[35] which was directly spiked as probe into the WSP water. $^1O_2$, ^3OM and $CO_3^{\cdot-}$ concentrations were determined based on the measured decay of probe compounds with known reaction rate constants, namely FFA ($k_{FFA-^1O_2}$ = $1.2 \cdot 10^8$ $M^{-1}s^{-1}$),[37] 2,4,6-trimethylphenol (TMP; k_{TMP-^3OM} = $4.8 \cdot 10^9$ $M^{-1}s^{-1}$)[41] and N,N-dimethylaniline (DMA, $k_{DMA-CO_3^{\cdot-}}$ = $1.85 \cdot 10^9$ $M^{-1}s^{-1}$),[42] respectively. The probe compounds were added at initial concentration in the range of 0.01 – 2.2 mM. The HPLC conditions used to monitor the time trends of the above compounds are given as SI.

Data analysis

Virus inactivation as well as probe compound degradation followed pseudo-first-order kinetics:

$$dc/dt = -k_{app} c \qquad \textbf{(EQ. 6)}$$

where c is the concentration of infective virus or probe compound, and k_{app} is the apparent pseudo-first-order inactivation or degradation rate constant. The values of k_{app} and their associated 95 % confidence intervals were determined from a least-square fit of $\ln(c/c_0)$ versus time.

If significant light shielding or dark inactivation occurred, k_{app} values were corrected accordingly prior to further data manipulation (see SI for details concerning light shielding corrections).

The time evolution of phenol formation from benzene could be approximated with the following equation:[41]

$$[Phenol] = \frac{k'_P [Benzene]_o}{k_P - k_B} (e^{-k_B t} - e^{-k_P t}) \qquad \textbf{(EQ. 7)}$$

where k'_P is the pseudo-first order rate constant of phenol formation from benzene, $[Benzene]_o$ the initial benzene concentration, k_P and k_B the pseudo-first order degradation rate constants of phenol and benzene, respectively. The initial formation rate of phenol is $R_P = k'_P [Benzene]_o$.

Results and discussion

Direct inactivation and inactivation quantum yields

Direct inactivation of MS2 proceeded at a five times slower rate compared to phiX174, and at an approximately equal rate as adenovirus (Fig. 1). Love et al.,[19] who also studied inactivation of phages and adenovirus type 2 by simulated sunlight, reported a comparable trend, though they found a larger (17-fold) difference between the inactivation rates of MS2 and adenovirus. Furthermore,

Shin et al.[43] showed that while adenovirus type 2 was more resistant to UV_{254} than MS2, its resistance diminished under the broader spectrum UV radiation of a medium pressure UV lamp. Similarly, the broad UV spectrum of simulated sunlight used in this study resulted in comparable resistances of adenovirus and MS2.

The inactivation quantum yields determined in this study are shown in Table 1. These values correspond within a factor of three to those determined by Rauth[44] for MS2 and phiX174 at 280 nm. As phiX174 is inactivated faster than MS2 while adsorbing comparable amounts of light, its inactivation quantum yield is larger. Each photon absorbed by phiX174 is five times more likely to cause inactivation compared to MS2. In contrast, MS2 and adenovirus exhibited similar apparent inactivation rate constants, even though the longer genome of adenovirus absorbs significantly more light. The inactivation quantum yield is thus lower for adenovirus than for MS2. This can be rationalized by considering that, as a dsDNA virus, adenovirus can use its host's cellular machinery to repair genomic UV damage.[43,45,46] Compared to the ssDNA and RNA viruses, adenovirus can therefore sustain more genomic UV damage without becoming inactivated, resulting in a lower inactivation quantum yield.

Note that for simplicity, we made the assumption in eq. 2 that each photon absorbed had the same inactivation quantum yield. As literature data suggest, however, shorter wavelengths in the range considered exhibit a stronger inactivating effect that longer ones[44]. Nevertheless, this approach was used because differences in inactivation quantum yields are rather small in the UVB range of sunlight spectrum (290-320 nm).[47]

Rate constants for indirect inactivation by reactive species

All three viruses were efficiently inactivated by all reactive species tested. An overview of the inactivation rate constants is given in Fig. 2, and exact values are listed in the SI (Table S4). For each reactive species, the virus susceptibility to inactivation followed the sequence MS2 > adenovirus > phiX174. The second-order rate constants for each virus were within one to two orders of magnitude. Below, the findings for each reactive species are discussed in detail.

Hydroxyl radical. $OH^{\cdot}$ exhibited second-order inactivation rate constants that were one to two orders of magnitude greater than those of the other reactive species (Fig. 2). As for many organic compounds, the inactivation rate constants were close to the diffusion limit. The most susceptible virus was MS2, which exhibited a $k_{MS2-OH^{\cdot}}$ of 7.4 (± 1.9)·10^9 $M^{-1}s^{-1}$. This high value was expected, given that $OH^{\cdot}$ are very reactive and MS2 is susceptible to oxidation.[23] The $k_{MS2-OH^{\cdot}}$ determined herein is comparable to that computed based on data by Mamane et al,[48] which yielded a value of 1.6·10^{10} $M^{-1}s^{-1}$. In contrast, the data reported by Rosado-Lausell et al.[49] suggest a nearly ten times greater $k_{MS2-OH^{\cdot}}$. This difference may stem from the fact that in their study, the $OH^{\cdot}$ concentration

used to calculate $k_{MS2-OH^{\cdot}}$ was determined in a separate reactor. This approach may introduce a significant error, as small differences in solution composition, such as the presence of a probe compound itself, can drastically change the steady-state concentration of a radical.

$k_{phiX174-OH^{\cdot}}$ was approximately four times smaller than $k_{MS2-OH^{\cdot}}$ (Fig. 2; SI, Table S4 and Fig. S1). This corresponds well to the data obtained by Sommer et al.,[23] who determined that inactivation of MS2 by ($OH^{\cdot}$ producing) ionizing radiation was six times more efficient than inactivation of phiX174. Finally, the susceptibility of adenovirus to $OH^{\cdot}$ lay between that of MS2 and phiX174, yielding a value of 4.2 (± 1.4)·10^9 $M^{-1}s^{-1}$. This was ten times larger than reported by Bounty et al. (4.6·10^{10} $M^{-1}s^{-1}$).[50] The higher value calculated by this group may result from synergistic effects between UV and $OH^{\cdot}$, as in their experimental set-up UV accounted for about 50 % of the inactivation. Under the conditions used herein, only about 1 % of inactivation was due to UV radiation.

Carbonate radical. For experiments with $CO_3^{\cdot-}$, the second-order rate constants were between 30 and 60 times smaller than the corresponding rate constants for $OH^{\cdot}$ (Fig 2, Table S4). This difference is not surprising, given that many building blocks of viruses (such as the amino acid residue tyrosine itself) exhibit a similar difference in their reactivity toward these two radicals[35,36] Furthermore, the three viruses had similar inactivation rate constants, within a factor of two. This indicates that the different viral structures and compositions had little influence on this inactivation mechanism. This can be rationalized by considering that $CO_3^{\cdot-}$ are more selective than $OH^{\cdot}$, and may react with similar targets on the three viruses. To our best knowledge, this is the first report of virus inactivation rate constants by $CO_3^{\cdot-}$.

Singlet oxygen. $k_{MS2-^1O_2}$ was about six times greater than $k_{phiX174-^1O_2}$ (Fig. 2, Table S4). The value for $k_{MS2-^1O_2}$ reported here (3.5 (± 0.3)·10^8 $M^{-1}s^{-1}$) corresponds well to those calculated based on previous studies (3.3-3.9·10^8 $M^{-1}s^{-1}$), where $^1O_2$ was also produced with Rose Bengal but by different excitation lamps.[18,49] Adenovirus was only slightly more resistant to $^1O_2$ than MS2 (Fig. 2, Table S4) which confirms that this virus is susceptible to oxidants. This data contradicts the statement of Dewilde et al.[51] that $^1O_2$ had no effect on non-enveloped viruses like adenovirus and poliovirus 1.

Additional experiments in D_2O were performed to confirm that in our experimental system inactivation was promoted by $^1O_2$ rather than the triplet state of the $^1O_2$-sensitizer Rose Bengal. Given a 2% content of H_2O in our experimental D_2O solutions and the 13-fold lower $^1O_2$ quenching rate constant of D_2O compared to H_2O, the k_{app} of both MS2 and phiX174 in D_2O should increase by a factor of 10.4 compared to the experiments conducted in H_2O. The observed increase in k_{app} was 6.7 ± 0.6 and 7.7 ± 1.7 for MS2 and phiX174, respectively (Table S4). The lower than expected

increase in k_{app} indicates that the triplet state of Rose Bengal contributes to inactivation. Nevertheless, as the contribution of the triplet state was small, we neglected it in the calculation of the second-order rate constants with $^1O_2$.

Triplet states. ^{3}AQ2S was markedly more efficient at inactivating MS2 compared to the other viruses; the corresponding second-order rate constant was 21 and 9-fold greater than for phiX174 and adenovirus, respectively (Fig. 2, Table S4). Hence, the difference in sensitivities of the three viruses toward ^{3}AQ2S was much greater than for the other reactive species tested. These results may indicate that the relevant targets of phiX174 and adenovirus are more easily accessible for small molecules, such as $^1O_2$ or $OH^{\cdot}$, than for a larger organic compound.

Rosado-Lausell et al.[49] studied MS2 inactivation and TMP degradation in the presence of the triplet sensitizer 3'-methoxyacetophenone. Based on these data, we computed a second-order rate constant of MS2 inactivation by triplet states of $1.62 \cdot 10^9$ $M^{-1}s^{-1}$, which is in good agreement with our result.

Overall, our results confirm previous findings that MS2, and to a lesser extent adenovirus, are relatively resistant to direct inactivation but are efficiently inactivated by oxidants. In contrast, phiX174 was more resistant to oxidants but readily underwent direct inactivation by UVB irradiation. Besides the type of genome, a major difference between MS2 and phiX174 is the structure of the capsid. The capsid of MS2 is thinner compared to that of phiX174 (21 Å vs. 30 Å, respectively),[52,53] and it contains pores. The thicker and more compact shell of phiX174 may provide it with greater oxidant scavenging ability, and may protect the genome by reducing the penetration of organic sensitizers and reactive species into the virus core. This hypothesis is consistent with findings by DeMik and DeGroot,[54] who reported that in the case of another oxidant, ozone, phiX174 was inactivated by protein damage, and that the nucleic acid was only secondarily affected. For MS2, in contrast, ozone has been suggested to mainly target the genome.[55]

Model to estimate and apportion inactivation processes in sunlit natural water

To validate the environmental relevance of the parameters derived above, we then determined if these parameters allowed us to estimate solar virus disinfection in an environmental water sample. Specifically, a simple model was formulated to estimate the virus inactivation rate:

$$dc_{virus}/dt = -k_{app} c_{virus} = -P_a^{virus} \Phi_v - \sum_{reactive\ species} k_{reactive\ species-virus} c_{reactive\ species,SS} c_{virus} \quad \text{(Eq. 8)}$$

To test this model, we determined the light penetration and steady-state concentrations of reactive species in a WSP sample, and used these data, combined with the kinetic parameters derived above (quantum yields and rate constants), to estimate virus inactivation. The estimated inactivation rate was then compared with the rate measured in the WSP sample.

In comparison with typical values for sunlit surface waters,[33,56] the WSP water exhibited similar steady-state concentrations upon irradiation by simulated sunlight, specifically: $OH^{\cdot}$ ($(1.76\pm0.80)\cdot10^{-16}$ M), $CO_3^{\cdot-}$ ($(3.4\pm2.1)\cdot10^{-15}$ M), $^1O_2$ ($(3.6\pm0.2)\cdot10^{-14}$ M) and ^3OM ($(4.7\pm2.4)\cdot10^{-15}$ M). This indicates that the photoreactivity of the organic matter in the WSP water used herein was comparable to that of other surface waters.

With the second-order inactivation rate constants, inactivation quantum yields and the steady-state concentrations of the reactive species in the WSP water in hand, the expected k_{app} in WSP water could be computed, according to Eq. 8. Finally, the computed k_{app} was compared to the experimentally determined one. As can be seen in Fig. 3, the computed k_{app} for all three viruses was lower than the experimentally observed one. The discrepancy between model and measurement was smallest for phiX174, for which nearly all inactivation was due to direct UVB absorption (97 % of the measured k_{app}). While our prediction for MS2 was also close to the measured one (11% difference), it was less accurate for adenovirus, for which the computed value underestimated the actual one by a factor of 6. This extensive inactivation of adenovirus may result from synergistic effects of different inactivation processes. For example, it has been shown that the combination of $^1O_2$ and hydrogen peroxide, which are both present in irradiated surface water, lead to faster MS2 inactivation that the sum of individual effects.[18] Adenovirus, which is a more complex virus than MS2, may undergo more pronounced synergisms, either between UV and reactive species or among reactive species. While further research is needed to elucidate and quantify such effects, synergisms may enhance adenovirus inactivation compared to the model presented in equation 8.

Surprisingly, the measured adenovirus inactivation was the most rapid of the three viruses, even though this virus is typically considered the most resistant organism to UV inactivation.[24–26] This behaviour may be due to the important role of oxidants in this WSP water. Specifically, $^1O_2$ has previously been found to degrade the protein domains of adenovirus associated with host attachment

and entry,[27] and other reactive species may attack the same sites. This type of damage prevents the virus from infecting the host, and hence renders it incapable of undergoing repair by the host machinery.

For the two phages, the estimated contribution of direct inactivation in our experimental set-up accounted for 53 and 95 % of the total measured inactivation of MS2 and phiX174, respectively. Furthermore, reactive species contributed only 2 % to the total inactivation of phiX174, while this contribution was 36 % for MS2. The remaining 3 % and 11 % of the measured k_{app} for phiX174 and MS2, respectively, could not be explained by processes described in Eq. 8. For both viruses, the most important reactive species predicted by our model was $^1O_2$. It accounted for 72 and 78 % to the total inactivation caused by the reactive species (indirect inactivation) for MS2 and phiX174, respectively. This is consistent with findings by Kohn and Nelson, who reported that $^1O_2$ was the main reactive species involved in the inactivation of MS2 in a Californian WSP.[18] Other reactive species contributed to the indirect MS2 inactivation in the following sequence: ^{3}OM (18 %), $OH^{\cdot}$ (7 %) and $CO_3^{\cdot-}$ (3 %). For phiX174 the order was different, with $OH^{\cdot}$ (11 %) contributing more than $CO_3^{\cdot-}$ (8 %) and ^{3}OM (3 %).

Inactivation that was unaccounted for by Eq. 8 can be rationalized by several possibilities. First, the missing fractions of inactivation may be due to synergistic effects not captured by the model, as discussed for adenovirus above. Alternatively, inaccurate measurements of reactive species concentrations may be implicated. Specifically, steady-state concentrations are highest close to the production source. For example, $^1O_2$ concentrations have been shown to be elevated in the close vicinity of OM compared to the bulk solution.[57] Hence, if OM adsorbs to MS2 or phiX174, the $^1O_2$ concentration the viruses are exposed to would be higher than the one measured in the bulk solution by the probe compounds used herein.[58] Finally, other reactive species may form in the sunlit pond water, such as superoxide, hydrogen peroxide or OM-derived radicals,[16] which may also contribute to virus inactivation but were not included in the model.

To conclude, this work elucidates pathways that lead to solar disinfection of three viruses in a waste stabilisation pond. MS2 is relatively resistant to UVB light; it may therefore be a conservative indicator of virus inactivation in surface waters where direct inactivation is the most important process. This would be the case in waters that contain little organic matter, where UVB light is readily transmitted and the production of oxidants is low. The phage phiX174, which is relatively resistant to oxidants, may serve as a conservative indicator in waters that contain high concentrations of organic matter, and that efficiently shield UVB light. The fast inactivation of adenovirus could not be explained by our analysis, but we propose that it was due to synergistic effects of the combined treatment of sunlight and oxidants that cause inactivation in sunlight surface waters. Future studies will elucidate if other human viruses can be more accurately captured by our model.

Finally, in order to further standardize experimental protocols, we suggest to use MS2 as a reference organism to study solar disinfection for different viruses. This approach offers two main advantages. First, MS2 is easy to work with and is already broadly used in many research groups. Second, it is susceptible to reactive species, which may greatly vary in concentration between water samples. Systematically including MS2 inactivation as a reference measurement would thus allow to standardize and interpret disinfection experiments with other viruses, even if different waters with varying characteristics are used.

Associated content

Supporting information: a list of chemicals and microorganisms; experimental details for HPLC analyses; correction for light shielding; experimental details and data pertaining to determination of second-order rate constants; determination of steady-state concentrations of reactive species in WPS water; spectra of Pyrex cell, solar simulator, MS2 and WSP water; light extinction spectra of viruses; tables of second-order rate constants of viruses inactivation by reactive species. This material is available free of charge via the Internet at http://pubs.acs.org/.

Acknowledgements

This work was supported by EPFL and the Swiss National Science Foundation (project no. 200020_131918). The authors thank Sylvain Coudret and Elena Rossel for laboratory assistance.

References

(1) Maynard, H.; Ouki, S.; Williams, S. Tertiary lagoons: a review of removal mecnisms and performance. *Water Res.* **1999**, *33*.

(2) Davies-Colley, R. *Pond disinfection*; Shilton, A., Ed.; IWA Publishing: London, 2005.

(3) Davies-Colley, R. J.; Donnison, A. M.; Speed, D. J. Towards a mechanistic understanding of pond disinfection. *Water Sci. Technol.* **2000**, *42*, 149–158.

(4) Calkins, J.; Buckles, J. D.; Moeller, J. R. Role of solar ultraviolet-radiation in natural-water purification. *Photochem. Photobiol.* **1976**, *24*, 49–57.

(5) Curtis, T. P.; Mara, D. D.; Silva, S. A. The effect of sunlight on fecal-coliforms in ponds - implications of research and design. *Water Sci. Technol.* **1992**, *26*, 1729–1738.

(6) Curtis, T. P.; Mara, D. D.; Silva, S. A. Influence of pH, Oxygen, and Humic Substances on Ability of Sunlight To Damage Fecal Coliforms in Waste Stabilization Pond Water. *Appl. Environ. Microbiol.* **1992**, *58*, 1335–1343.

(7) Davies-Colley, R. J.; Donnison, A. M.; Speed, D. J.; Ross, C. M.; Nagels, J. W. Inactivation of faecal indicator micro-organisms in waste stabilisation ponds: interactions of environmental factors with sunlight. *Water Res.* **1999**, *33*, 1220–1230.

(8) Reed, R. H. The inactivation of microbes by sunlight: Solar disinfection as a water treatment process. *Adv. Appl. Microbiol. Vol 54* **2004**, *54*, 333–365.

(9) Sinton, L. W.; Finlay, R. K.; Lynch, P. A. Sunlight inactivation of fecal bacteriophages and bacteria in sewage-polluted seawater. *Appl. Environ. Microbiol.* **1999**, *65*, 3605–3613.

(10) Sinton, L.; Hall, C.; Lynch, P. A.; Davies-Colley, R. J. Sunlight inactivation of fecal indicator bacteria and bacteriophages from waste stabilization pond effluent in fresh and saline waters. *Appl. Environ. Microbiol.* **2002**, *68*, 1122–1131.

(11) McGuigan, K. G.; Conroy, R. M.; Mosler, H.-J.; du Preez, M.; Ubomba-Jaswa, E.; Fernandez-Ibañez, P. Solar water disinfection (SODIS): a review from bench-top to roof-top. *J. Hazard. Mater.* **2012**, *235-236*, 29–46.

(12) Wegelin, M.; Canonica, S.; Mechsner, K.; Fleischmann, T.; Pesaro, F.; Metzler, A. Solar water disinfection: scope of the process and analysis of radiation experiments. *J. Water Supply Res. Technol.* **1994**, *43*, 154–169.

(13) Castillo, G. C.; Trumper, B. A. Coliphages and other microbial indicators in stabilization ponds. *Environ. Toxicol. Water Qual.* **1991**, *6*, 197–207.

(14) Davies-Colley, R. J.; Craggs, R. J.; Park, J.; Sukias, J. P. S.; Nagels, J. W.; Stott, R. Virus removal in a pilot-scale “advanced” pond system as indicated by somatic and F-RNA bacteriophages. *Water Sci. Technol.* **2005**, *51*, 107–110.

(15) Boule, P.; Hutzinger, O. *Environmental Photochemistry*; Springer-Verlag: Berlin, 1999; Vol. 2 L, p. xi, 359 p.

(16) Boule, P.; Bahnemann, D. W.; Robertson, P. K. J. *Environmental Photochemistry Part II*; Springer Verlag: Berlin, 2005; Vol. 2 M, p. xi, 489 p.

(17) Davies-Colley, R. J.; Donnison, A. M.; Speed, D. J. Sunlight wavelengths inactivating faecal indicator microorganisms in waste stabilisation ponds. *Water Sci. Technol.* **1997**, *35*, 219–225.

(18) Kohn, T.; Nelson, K. L. Sunlight-mediated inactivation of MS2 coliphage via exogenous singlet oxygen produced by sensitizers in natural waters. *Environ. Sci. Technol.* **2007**, *41*, 192–197.

(19) Love, D. C.; Silverman, A.; Nelson, K. L. Human Virus and Bacteriophage Inactivation in Clear Water by Simulated Sunlight Compared to Bacteriophage Inactivation at a Southern California Beach. *Environ. Sci. Technol.* **2010**, *44*, 6965–6970.

(20) Romero, O. C.; Straub, A. P.; Kohn, T.; Nguyen, T. H. Role of Temperature and Suwannee River Natural Organic Matter on Inactivation Kinetics of Rotavirus and Bacteriophage MS2 by Solar Irradiation. *Environ. Sci. Technol.* **2011**, *45*, 10385–10393.

(21) Silverman, A. I.; Peterson, B. M.; Boehm, A. B.; McNeill, K.; Nelson, K. L. Sunlight Inactivation of Human Viruses and Bacteriophages in Coastal Waters Containing Natural Photosensitizers. *Environ. Sci. Technol.* **2013**, *47*, 1870–1878.

(22) Romero-Maraccini, O. C.; Sadik, N. J.; Rosado-Lausell, S. L.; Pugh, C. R.; Niu, X.-Z.; Croué, J.-P.; Nguyen, T. H. Sunlight-induced inactivation of human Wa and porcine OSU rotaviruses in the presence of exogenous photosensitizers. *Environ. Sci. Technol.* **2013**, *47*, 11004–11012.

(23) Sommer, R.; Pribil, W.; Appelt, S.; Gehringer, P.; Eschweiler, H.; Leth, H.; Cabaj, A.; Haider, T. Inactivation of bacteriophages in water by means of non-ionizing (UV-253.7 nm) and ionizing (gamma) radiation: A comparative approach. *Water Res.* **2001**, *35*, 3109–3116.

(24) Meng, Q. S.; Gerba, C. P. Comparative inactivation of enteric adenoviruses, poliovirus and coliphages by ultraviolet irradiation. *Water Res.* **1996**, *30*, 2665–2668.

(25) Gerba, C. P.; Gramos, D. M.; Nwachuku, N. Comparative inactivation of enteroviruses and adenovirus 2 by UV light. *Appl. Environ. Microbiol.* **2002**, *68*, 5167–5169.

(26) Nwachuku, N.; Gerba, C. P.; Oswald, A.; Mashadi, F. D. Comparative inactivation of adenovirus serotypes by UV light disinfection. *Appl. Environ. Microbiol.* **2005**, *71*, 5633–5636.

(27) Bosshard, F.; Armand, F.; Hamelin, R.; Kohn, T. Mechanisms of human adenovirus inactivation by sunlight and UVC light as examined by quantitative PCR and quantitative proteomics. *Appl. Environ. Microbiol.* **2013**, *79*, 1325–1332.

(28) Gallagher, S. R. Quantitation of DNA and RNA with absorption and fluorescence spectroscopy. In *Current Protocols in Molecular Biology*; John Wiley & Sons, Inc., 2011; Vol. Supplement.

(29) Borodavka, A.; Tuma, R.; Stockley, P. G. Evidence that viral RNAs have evolved for efficient, two-stage packaging. *Proc. Natl. Acad. Sci. U. S. A.* **2012**, *109*, 15769–15774.

(30) The Scripps Research Institute. Oligo Extinction Coefficient Calculator https://www.scripps.edu/california/research/dna-protein-research/forms/biopolymercalc2.html.

(31) Sanger, F.; Air, G. M.; Barrell, B. G.; Brown, N. L.; Coulson, A. R.; Fiddes, J. C.; Hutchison, C. A.; Slocombe, P. M.; Smith, M. Nucleotide sequence of bacteriophage [phi]X174 DNA. *Nature* **1977**, *265*, 687–695.

(32) National Center for Biotechnology Information http://www.ncbi.nlm.nih.gov/.

(33) Schwarzenbach, R. P.; Gschwend, P. M.; Imboden, D. M. *Environmental Organic Chemistry*; 2nd ed.; Wiley: Hoboken, N.J., 2003; p. xiii, 1313 p.

(34) Vione, D.; Minella, M.; Maurino, V.; Minero, C. Indirect photochemistry in sunlit surface waters: Photoinduced production of reactive transient species. *Chemistry Eur. J.* **2014**, *20*, 10590-10606.

(35) Buxton, G. V; Greenstock, C. L.; Helman, W. P.; Ross, A. B. Critical-review of rate constants for reactions of hydrated electrons, hydrogen-atoms and hydroxyl radicals (.OH/.O-) in aqueous-solution. *J. Phys. Chem. Ref. Data* **1988**, *17*, 513–886.

(36) Neta, P.; Huie, R. E.; Ross, A. B. Rate constants for reactions of inorganic radicals in aqueous-solution. *J. Phys. Chem. Ref. Data* **1988**, *17*, 1027–1284.

(37) Halladja, S.; Ter Halle, A.; Aguer, J.-P.; Boulkamh, A.; Richard, C. Inhihition of humic substances mediated photooxygenation of furfuryl alcohol by 2,4,6-trimethylphenol. Evidence for reactivity of the phenol with humic triplet excited states. *Environ. Sci. Technol.* **2007**, *41*, 6066–6073.

(38) Rodgers, M. A. J.; Snowden, P. T. Lifetime of O2(1Δg) in liquid water as determined by time-resolved infrared luminescence measurements. *J. Am. Chem. Soc.* **1982**, *104*, 5541–5543.

(39) Loeff, I.; Treinin, A.; Linschitz, H. Photochemistry of 9,10-antraquinone-2-sulfonate in solution. 1. Intermediates and mechanism. *J. Phys. Chem.* **1983**, *87*, 2536–2544.

(40) Maddigapu, P. R.; Bedini, A.; Minero, C.; Maurino, V.; Vione, D.; Brigante, M.; Mailhot, G.; Sarakha, M. The pH-dependent photochemistry of anthraquinone-2-sulfonate. *Photochem. Photobiol. Sci.* **2010**, *9*, 323–330.

(40a) Ruggeri, G.; Ghigo, G.; Maurino, V.; Minero, C.; Vione, D. Photochemical transformation of ibuprofen into harmful 4-isobutylacetophenone: Pathways, kinetics, and significance for surface waters. *Wat. Res.* **2013**, *47*, 6109-6121.

(41) De Laurentiis, E.; Buoso, S.; Maurino, V.; Minero, C.; Vione, D. Optical and photochemical characterization of chromophoric dissolved organic matter from lakes in Terra Nova Bay, Antarctica. Evidence of considerable photoreactivity in an extreme environment. *Environ. Sci. Technol.* **2013**, *47*, 14089-14098.

(42) Canonica, S.; Kohn, T.; Mac, M.; Real, F. J.; Wirz, J.; Von Gunten, U. Photosensitizer method to determine rate constants for the reaction of carbonate radical with organic compounds. *Environ. Sci. Technol.* **2005**, *39*, 9182–9188.

(43) Shin, G.-A.; Lee, J.-K.; Linden, K. G. Enhanced effectiveness of medium-pressure ultraviolet lamps on human adenovirus 2 and its possible mechanism. *Water Sci. Technol.* **2009**, *60*, 851–857.

(44) Rauth, A. M. Physical State of Viral Nucleic Acid and Sensitivity of Viruses to Ultraviolet Light. *Biophys. J.* **1965**, *5*, 257–273.

(45) Rainbow, A. J.; Mak, S. DNA damage and biological function of human Adenovirus after UV-irradiation. *Int. J. Radiat. Biol.* **1973**, *24*, 59–72.

(46) Beck, S. E.; Rodriguez, R. A.; Linden, K. G.; Hargy, T. M.; Larason, T. C.; Wright, H. B. Wavelength Dependent UV Inactivation and DNA Damage of Adenovirus as Measured by Cell Culture Infectivity and Long Range Quantitative PCR. *Environ. Sci. Technol.* **2014**, *48*, 591–598.

(47) Setlow, R.; Boyce, R. The Ultraviolet Light Inactivation of Bacteriophage-phi-X174 at different Wave Lengths and pHs. *Biophys. J.* **1960**, *1*, 29–41.

(48) Mamane, H.; Shemer, H.; Linden, K. G. Inactivation of E-coli, B-subtilis spores, and MS2, T4, and T7 phage using UV/H2O2 advanced oxidation. *J. Hazard. Mater.* **2007**, *146*, 479–486.

(49) Rosado-Lausell, S. L.; Wang, H.; Gutierrez, L.; Romero-Maraccini, O. C.; Niu, X.-Z.; Gin, K. Y. H.; Croue, J.-P.; Nguyen, T. H. Roles of singlet oxygen and triplet excited state of dissolved organic matter formed by different organic matters in bacteriophage MS2 inactivation. *Water Res.* **2013**, *47*, 4869–4879.

(50) Bounty, S.; Rodriguez, R. A.; Linden, K. G. Inactivation of adenovirus using low-dose UV/H2O2 advanced oxidation. *Water Res.* **2012**, *46*, 6273–6278.

(51) Dewilde, A.; Pellieux, C.; Hajjam, S.; Wattre, P.; Pierlot, C.; Hober, D.; Aubry, J. M. Virucidal activity of pure singlet oxygen generated by thermolysis of a water-soluble naphthalene endoperoxide. *J. Photochem. Photobiol. B-Biology* **1996**, *36*, 23–29.

(52) Kuzmanovic, D. A.; Elashvili, I.; Wick, C.; O'Connell, C.; Krueger, S. The MS2 coat protein shell is likely assembled under tension: A novel role for the MS2 bacteriophage A protein as revealed by small-angle neutron scattering. *J. Mol. Biol.* **2006**, *355*, 1095–1111.

(53) McKenna, R.; Xia, D.; Willingmann, P.; Ilag, L. L.; Krishnaswamy, S.; Rossmann, M. G.; Olson, N. H.; Baker, T. S.; Incardona, N. L. Atomic-Structure of Single-Stranded-DNA Bacteriophage-phi-X174 and its Functional Implications. *Nature* **1992**, *355*, 137–143.

(54) Demik, G.; Degroot, I. Mechanisms of inactivation of bacteriophage PSI-X174 and its DNA in aerosols by ozone and ozonized cyclohexene. *J. Hyg. (Lond).* **1977**, *78*, 199–211.

(55) Shin, G. A.; Sobsey, M. D. Reduction of Norwalk virus, poliovirus 1, and bacteriophage MS2 by ozone disinfection of water. *Appl. Environ. Microbiol.* **2003**, *69*, 3975–3978.

(56) Sulzberger, B.; Canonica, S.; Egli, T.; Giger, W.; Klausen, J.; von Gunten, U. Oxidative transformations of contaminants in natural and in technical systems. *Chimia (Aarau).* **1997**, *51*, 900–907.

(57) Latch, D.; McNeill, K. Microheterogeneity of singlet oxygen distributions in irradiated humic acid solutions. *Science (80-.).* **2006**, *311*, 1743–1747.

(58) Kohn, T.; Grandbois, M.; McNeill, K.; Nelson, K. L. Association with natural organic matter enhances the sunlight-mediated inactivation of MS2 coliphage by singlet oxygen. *Environ. Sci. Technol.* **2007**, *41*, 4626–4632.

Tables and figures

TABLE 1: QUANTUM YIELD FOR DIRECT INACTIVATION BY SUNLIGHT FOR MS2, PHIX174 AND ADENOVIRUS. VALUES ARE REPORTED WITH 95 % CONFIDENCE INTERVALS.

Φ_{MS2} [pfu inactivated/ photon absorbed]	$\Phi_{phiX174}$ [pfu inactivated / photon absorbed]	$\Phi_{Adenovirus}$ [pfu inactivated / photon absorbed]
$(2.9\pm 0.4)\cdot 10^{-3}$	$(1.42\pm 0.10)\cdot 10^{-2}$	$(2.5\pm 0.5)\cdot 10^{-4}$

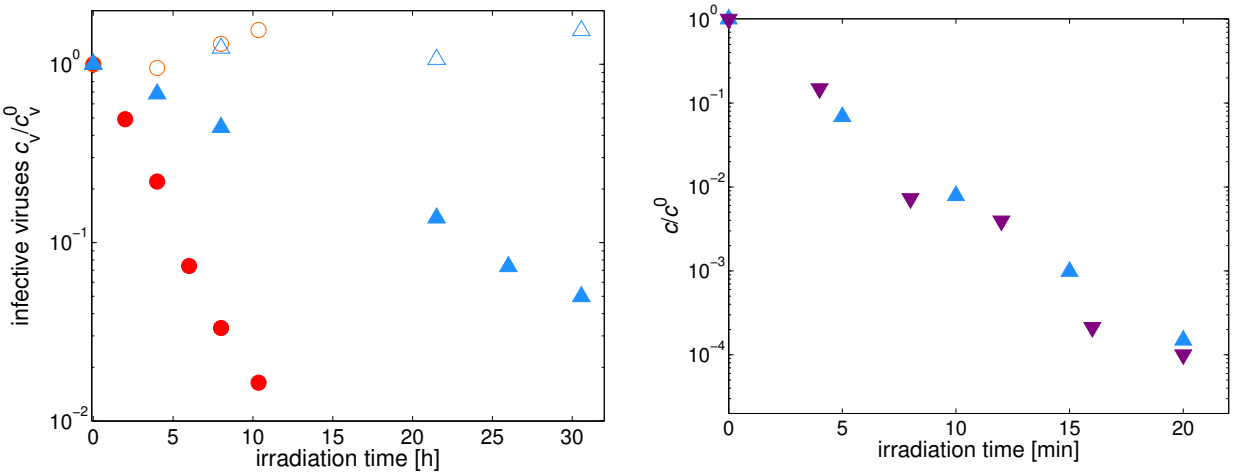

FIGURE 1: INACTIVATION EXPERIMENTS CONDUCTED IN PBS UNDER THE SOLAR SIMULATOR. (LEFT) INACTIVATION OF PHIX174 (●) AND MS2 (▲) WITH THE AE FILTER OR IN THE DARK (EMPTY SYMBOLS). (RIGHT) INACTIVATION OF MS2 (▲) AND ADENOVIRUS (▼) WITHOUT THE AE FILTER.

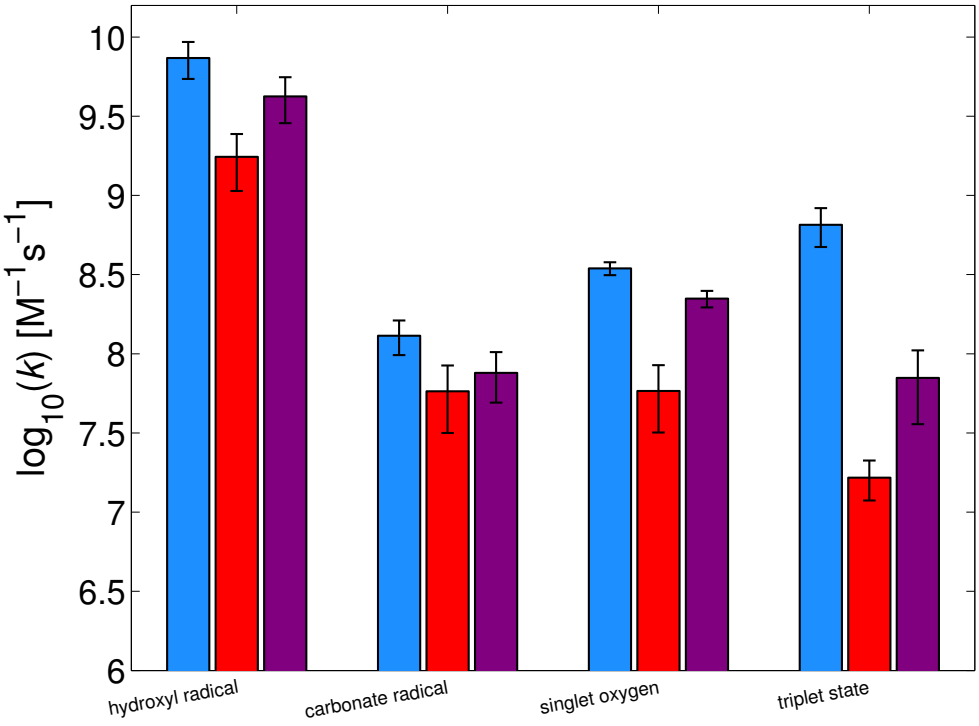

FIGURE 2: SECOND-ORDER INACTIVATION RATE CONSTANTS OF MS2 (BLUE), PHIX174 (RED) AND ADENOVIRUS (PURPLE) WITH HYDROXYL AND CARBONATE RADICALS, SINGLET OXYGEN AND TRIPLET STATES. VALUES ARE REPORTED WITH 95 % CONFIDENCE INTERVALS.

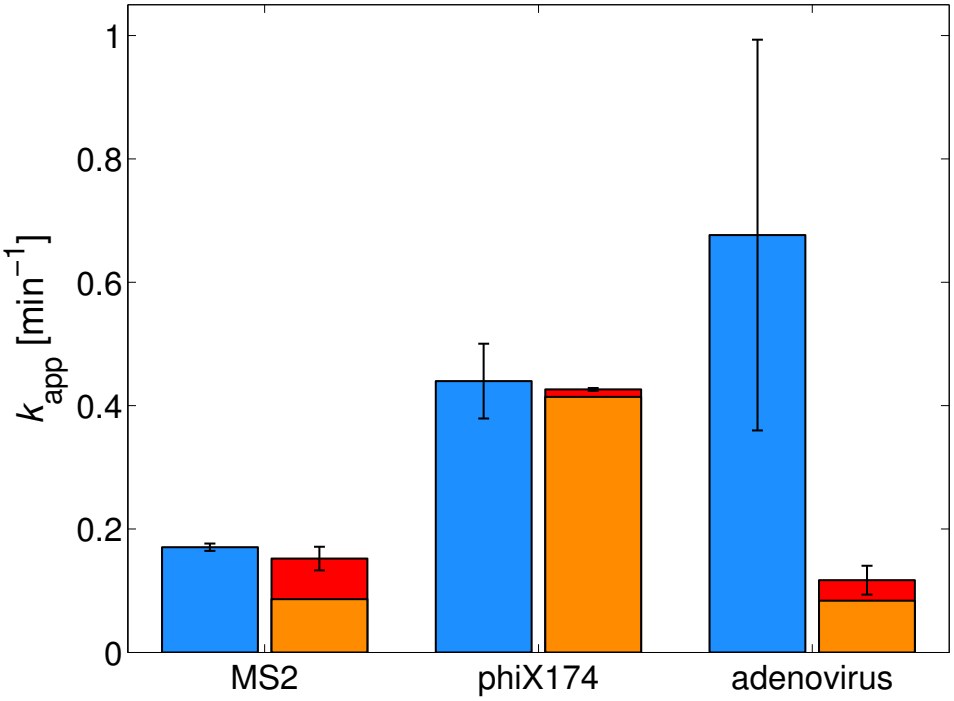

FIGURE 3: MEASURED (BLUE) AND COMPUTED APPARENT INACTIVATION RATE CONSTANTS k_{APP} (RED/ORANGE, EQ. 8) FOR MS2, PHIX174 AND ADENOVIRUS FROM EXPERIMENTS PERFORMED UNDER THE SOLAR SIMULATOR. THE ORANGE PORTION OF THE BAR INDICATES THE CONTRIBUTION OF DIRECT INACTIVATION, CALCULATED USING EQ. 1 AND THE QUANTUM YIELDS (TABLE 1). THE RED PORTION INDICATES THE CONTRIBUTION OF INDIRECT INACTIVATION, CALCULATED BASED ON THE SECOND-ORDER INACTIVATION RATE CONSTANTS (FIGURE 2) AND THE MEASURED STEADY-STATE CONCENTRATIONS OF THE FOUR REACTIVE SPECIES (TABLE S4).